Ab-initio calculations of the Ruddlesden–Popper phases $CaMnO_3$, $CaO(CaMnO_3)$ and $CaO(CaMnO_3)_2$

2008 J. Phys.: Condens. Matter 20 035202

(http://iopscience.iop.org/0953-8984/20/3/035202)

J. Phys.: Condens. Matter **20** (2008) 035202 (8pp) doi:10.1088/0953-8984/20/03/035202

Ab-initio calculations of the Ruddlesden–Popper phases $CaMnO_3$, $CaO(CaMnO_3)$ and $CaO(CaMnO_3)_2$

C Cardoso[1], R P Borges[2], T Gasche[2,3] and M Godinho[2,4]

[1] CFC, Physics Department, University of Coimbra, 3004-516 Coimbra, Portugal
[2] Centro de Física da Matéria Condensada - Universidade de Lisboa, Campo Grande, Ed. C8, 1749-016, Lisboa, Portugal
[3] CINAMIL Laboratório de Física, Academia Militar, Lisboa, Portugal
[4] Departamento de Física, Faculdade de Ciências, Universidade de Lisboa, Campo Grande, Ed. C8, 1749-016, Lisboa, Portugal

E-mail: cmcardoso@teor.fis.uc.pt

Received 3 July 2007, in final form 11 October 2007
Published 10 December 2007
Online at stacks.iop.org/JPhysCM/20/035202

Abstract

The present work reports *ab-initio* density functional theory calculations for the Ruddlesden–Popper phase $CaO(CaMnO_3)_n$ compounds. In order to study the evolution of the properties with the number of perovskite layers, a detailed analysis of the densities of states calculated for each compound and for several magnetic configurations was performed. The effect of distortions of the crystal structure on the magnetic ground state is also analysed and the exchange constants and transition temperatures are calculated for the three compounds using a mean field model. The calculated magnetic ground state structures and magnetic moments are in good agreement with experimental results and previous calculations.

1. Introduction

Transition metal oxides, in particular perovskite type structures like the Ruddlesden–Popper (R–P) phases, exhibit a rich variety of electronic properties such as insulator–metal transitions, superconductivity and charge ordering [1]. The complex physical processes involved in these phenomena are the result of the interactions between spin, charge and structural degrees of freedom. Researchers have focused their attention on these compounds due to their potential technological applications in superconducting devices, ferroelectric memories or even magnetic sensors since some of them also exhibit colossal magnetoresistance.

Perovskites are described by the formula ABO_3, where A is a rare-earth or an alkaline-earth and B a transition metal. The crystal structure is cubic or nearly cubic, with O forming octahedra around B centres. The Ruddlesden–Popper phases alternate blocks of perovskite cells with a single A–O layer that decouples electrically and magnetically the perovskite blocks [2]. The R–P phases' generic formula is $AO(ABO_3)_n$, with n the number of octahedra layers within a perovskite block, where the perovskite structure is described by $n = \infty$. The present work is focused on manganese oxides of the type $CaO(CaMnO_3)_n$ where $n = 1$, 2 and ∞. Their crystal structures are illustrated in figure 1.

According to the results reported in [3], $CaO(CaMnO_3)$ and $CaO(CaMnO_3)_2$ crystallize in tetragonal structures, $I4_1/acd$ and $I4/mmm$ respectively and $CaMnO_3$ has an orthorhombic structure corresponding to a small distortion of the cubic $Pnma$ structure. The fact that the sum of atomic radii in the Mn–O layers, $R_{Mn} + R_O \sim 190$ pm, differs from the corresponding distance in the Ca–O layers, $(R_{Ca} + R_O)/\sqrt{2} \sim 160$ pm justifies the distortion.

Antiferromagnetic order is observed in the three compounds with magnetic moments close to 2.5 μ_B/Mn [3, 4], a value that is lower than that expected for the Mn^{4+} ion, 3.9 μ_B [5]. The transition temperature does not decrease significantly with n, being 125 K for $CaMnO_3$ and 110 K for $CaO(CaMnO_3)$ and $CaO(CaMnO_3)_2$. Resistivity, however, increases for compounds with lower n, due to the introduction of insulating layers between the perovskite blocks. The gap energies for $CaMnO_3$, $CaO(CaMnO_3)_2$ and $CaO(CaMnO_3)$ are respectively 0.06, 0.13 and 0.14 eV [3]. *Ab-initio* calculations performed for $CaMnO_3$ determined, in agreement with the experimental data, an insulating type G antiferromagnetic ground state configuration. The

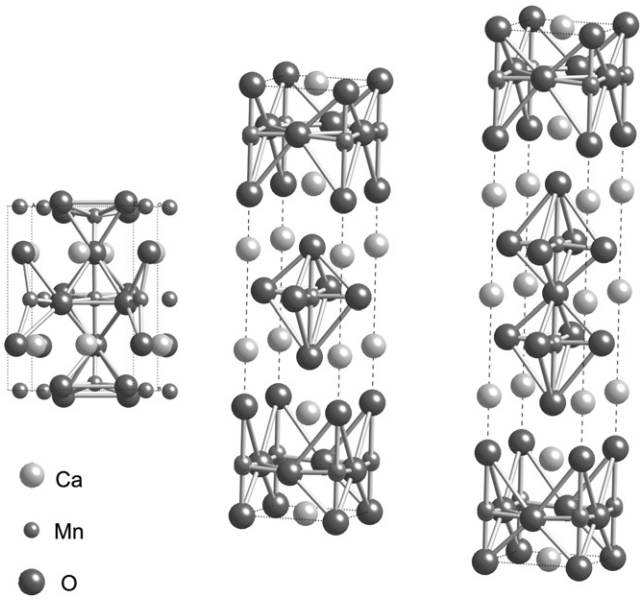

Figure 1. Crystal structures of $CaO(CaMnO_3)_n$ for $n = \infty$ on the left, $n = 1$ at the centre and $n = 2$ on the right-hand side.

calculated insulating gap is 0.42 eV and the magnetic moment 2.48 μ_B/Mn [6].

These three compounds represent a trend from three-dimensional $CaMnO_3$ to two-dimensional $CaO(CaMnO_3)$ but they all have very similar ordering temperatures, around 100 K. As discussed in [7] the overlap integrals in these compounds are close to a crossover value that separates the localized from the itinerant antiferromagnetic regimes. Within this condition, since the exchange constant is especially sensitive to the lattice parameter, reduction of the lattice parameter could compensate for the reduction of the number of neighbours. According to this reference, the small differences in the cation–anion–cation distance have a considerable influence on the magnitude of the exchange interaction, which should be largest for $CaO(CaMnO_3)_2$ and larger for $CaO(CaMnO_3)$ than for $CaMnO_3$. The Curie–Weiss temperatures found experimentally are *anomalously* higher than the ordering temperatures, decreasing with increasing n: 1037 K for $CaO(CaMnO_3)$, 714 K for $CaO(CaMnO_3)_2$ and 511 K for $CaMnO_3$ [3].

As discussed in [8], the increasing two-dimensional magnetic fluctuations as n decreases and approaches a two-dimensional structure is consistent with the measured high temperature magnetic behaviour. However, the three-dimensional perovskite $CaMnO_3$ already shows an anomalously high Curie–Weiss temperature and low magnetic response at high temperature. Therefore the authors question the role of the two-dimensional fluctuations and the suggestion by Goodenough [7] that covalency induces loss of local moment behaviour.

2. Calculation

In order to understand the evolution of the electronic properties with n we performed an *ab-initio* study on the Ruddlesden–Popper phases $CaO(CaMnO_3)_n$, $n = 1, 2, \infty$. Our calculations, based on density functional theory, within the local density approximation, were performed using the augmented spherical waves (ASW) method [9, 10]. The Ca and Mn 4s, 4p and 3d, and O 2p, 2d and 3d states were treated as valence states, and the low-lying O 2s states as core states. ASW spheres of radii 2, 2.6 and 3.4 Å were used for O, Mn and Ca respectively. The energy and magnetic moments were converged below 10^{-4} eV and 10^{-4} μ_B, respectively. The calculations were performed with a grid of $6 \times 6 \times 6$ reciprocal lattice points. Convergence with respect to the number of k-points was confirmed with a $10 \times 10 \times 10$ grid. The total energy difference is below the energy convergent parameter and the magnetic moment changes less than 3×10^{-4} μ_B. No empty spheres were used in the present calculation. For the calculation of the exchange constants and transition temperatures, the ferromagnetic and several antiferromagnetic structures were considered.

3. Results and discussion

In the following paragraphs we will describe the calculated density of states for the three mentioned compounds. As we will show below there are some generic features that are present in all the densities of states. In the next sections we will analyse in detail all the densities of states calculated for $CaMnO_3$. For the sake of simplicity, the results for the other two compounds will be described more briefly.

3.1. $CaMnO_3$

We begin the study of R–P compounds by the end of the series, the perovskite corresponding to $n = \infty$. In figure 2 the paramagnetic density of states (DOS) is plotted for the *Pnma* orthorhombic crystal structure [3]: the top plot shows the total density of states and the following, the partial densities of Mn, Ca and O. The Fermi level, $E = 0$, lies in the centre of a t_{2g} Mn band, separated from the e_g band by a gap of 0.2 eV, 0.7 eV above E_F. The O and Ca states extend to lower energies, below −1.4 eV Mn, Ca and O densities of states have similar shapes, reflecting a strong hybridization. The Mn states give a large contribution to the density of states at the Fermi level that, according to the Stoner criteria, would lead to a significant spin moment in the magnetic cases.

The ferromagnetic density of states for the orthorhombic structure plotted in figure 3, shows a gap width of 0.3 eV. The Mn moment is found to be 2.61 μ_B. The hybridization between Mn and O states decreases the electronic density in the Mn 3d band, explaining the lower moment when compared with the Mn^{4+} moment of 3.9 μ_B, obtained considering a half occupied t_{2g} band. Mn and O states, located at the same energy values, reflect the hybridization between the 2p O states and the 3d Mn states, leading to the presence of 2p states in the conduction band. The Ca and O bands show a spin splitting which results in a small O moment of 0.1 μ_B and Ca moment of less than 0.1 μ_B. The total moment is an integer value of 3.00 μ_B, as it should be for a magnetic insulator.

The experimental ground state is antiferromagnetic: three different antiferromagnetic states were analysed, namely

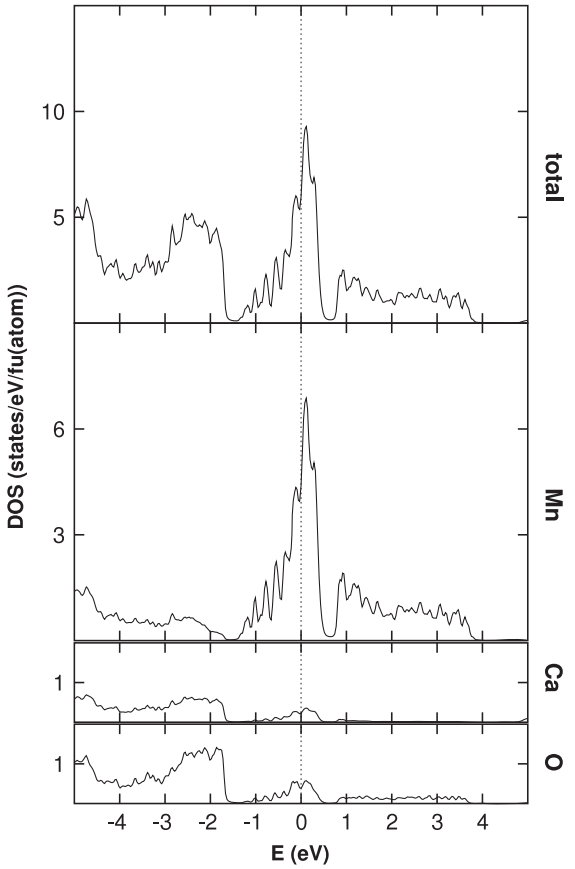

Figure 2. Densities of states calculated for the orthorhombic structure of $CaMnO_3$ in the paramagnetic state. The four plots represent the total density of states, and the Mn, Ca and O partial density of states.

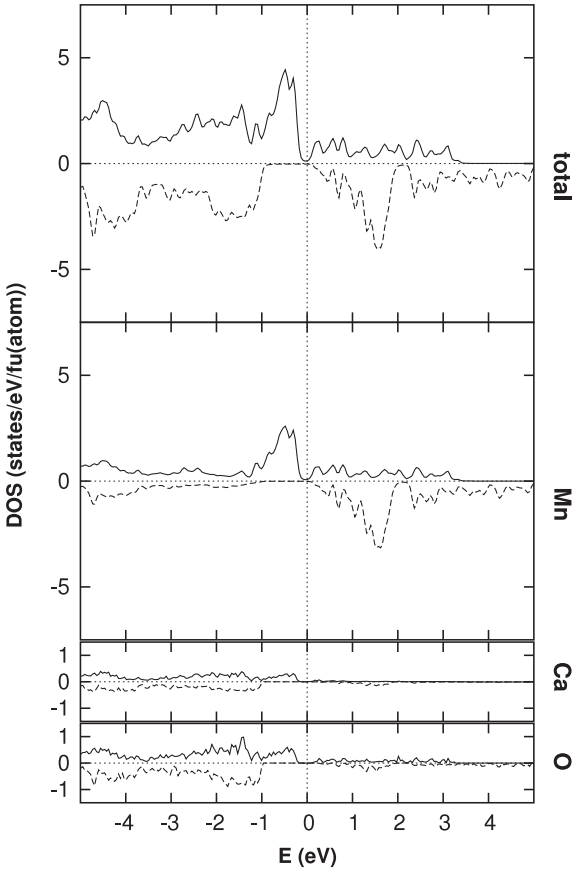

Figure 3. Densities of states calculated for the orthorhombic structure of $CaMnO_3$, in the ferromagnetic state. The plots represent the spin up (solid lines) and down (dashed lines) density of states, and the Mn, Ca and O partial density of states.

the A, C and G-type phases. The A C and G-type antiferromagnetic modes can be described, for a cubic structure, as consisting of antiferromagnetic coupled ferromagnetic planes of {001}, {110} and {111} respectively. In all of the cases studied the spin moments are aligned along the *c* axis.

Densities of states are similar for the three antiferromagnetic calculations, with the G-type having the lowest energy. Figure 4 shows density of states for the type G antiferromagnetic configuration with a 1.7 eV spin splitting of the Mn states. The crystal field value, estimated by the splitting of the e_g and t_{2g} states, is 1.7 eV and the energy gap, 0.4 eV. This leads to an insulating behaviour with the t_{2g} band completely polarized. Compared with the ferromagnetic calculation, in all the antiferromagnetic configurations the Ca and O atoms have zero moment. The wider densities of states in the antiferromagnetic calculations show an increase in hybridization, which results in a lower magnetic moment for the Mn atoms in the antiferromagnetic configurations.

The $CaMnO_3$ orthorhombic structure has two non-equivalent Mn–O distances of 1.92 and 1.89 Å and can be seen as a slight distortion of a cubic structure. In order to evaluate the role of such distortion, the density of states was also calculated for an idealized cubic cell. This cubic cell can be deduced by taking the average of the two Mn–O distances of the orthorhombic structure. The density of states for the cubic G-type antiferromagnetic configuration is presented in figure 5. The 0.4 eV gap in the Fermi level is very close to the orthorhombic case, and in good agreement with other values also calculated for a cubic structure [6]. The distribution of the bands is very similar to that of the orthorhombic compound. We should point out that x-ray diffraction data have also led to the determination of a cubic structure for $CaMnO_3$ [4]. This means the distortion is so small that one can expect it to have no significant impact on the magnetic ordering of the compound.

The calculated Mn magnetic moments for different configurations and crystal structures are summarized in table 1. The values range from 2.5 to 2.7 μ_B/Mn, and are close to previously reported values: 2.65 μ_B/Mn from neutron diffraction data [4], 2.48 μ_B/Mn, from LDA calculations for the type G antiferromagnetic cubic structure [6]. As mentioned above, antiferromagnetic configurations of both crystal structures show lower magnetic moments than the ferromagnetic configuration but both values are significantly lower than the Mn^{4+} moment. This is due to the Mn and O hybridization, which results in a broadening of the 3d states. In the case of the orthorhombic structure, the ferromagnetic and the type G antiferromagnetic configurations have respectively 0.31 and 0.44 eV/Mn less energy than the paramagnetic state. Therefore the antiferromagnetic configuration corresponds to

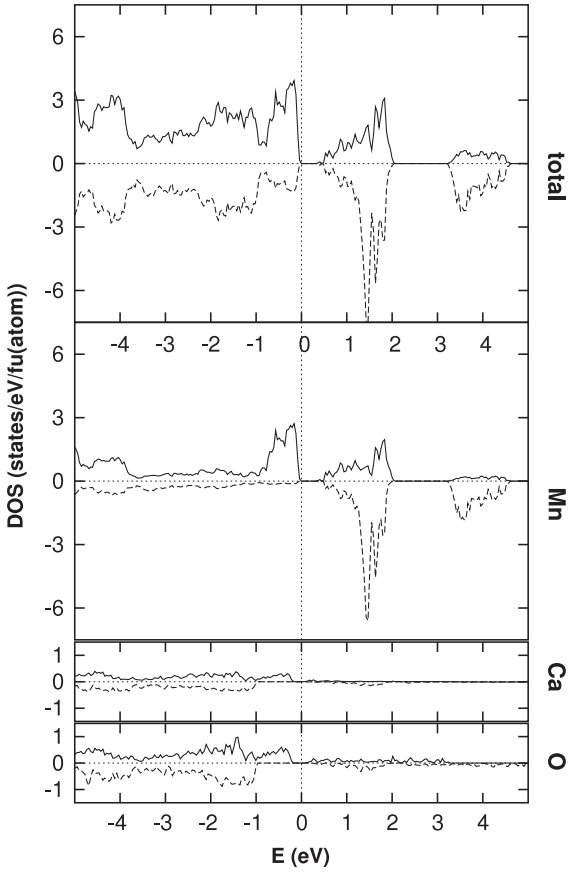

Figure 4. Densities of states calculated for an orthorhombic structure of $CaMnO_3$, in the type G antiferromagnetic state. The plots represent the spin up (solid lines) and down (dashed lines) total density of states, and the Mn, Ca and O partial density of states.

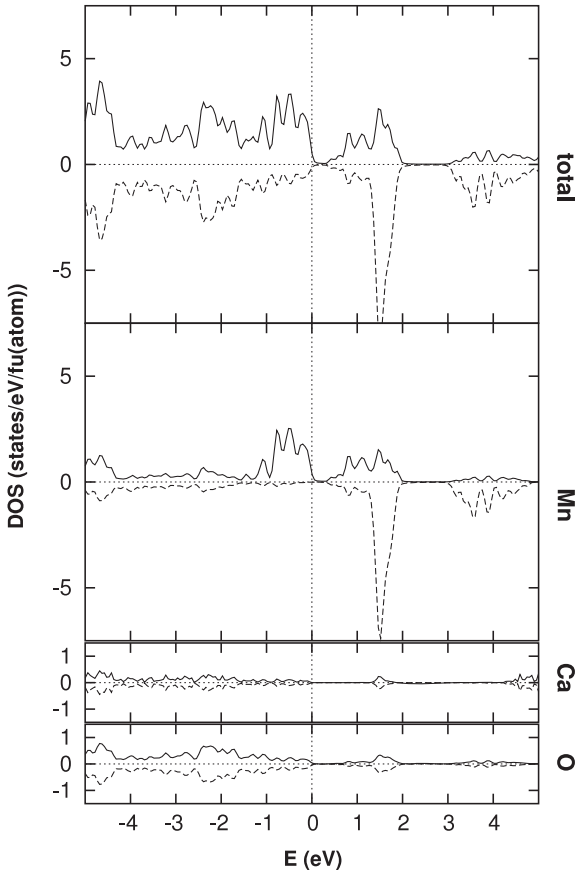

Figure 5. Densities of states of $CaMnO_3$, calculated for a cubic crystal structure and a type G antiferromagnetic configuration. The plots represent the spin up (solid lines) and down (dashed lines) density of states, and the Mn, Ca and O partial density of states.

Table 1. Magnetic moments and energy differences of cubic and orthorhombic (*Pnma*) $CaMnO_3$, for ferro and A-, C- and G-type antiferromagnetic configurations. For each crystal structure, the energy differences were calculated with respect to the corresponding paramagnetic state. The A-, C- and G-type antiferromagnetic modes can be described, for a cubic structure, as consisting of oppositely aligned ferromagnetic planes of {001}, {110} and {111}, respectively.

Crystal structure	Magnetic structure	m (μ_B/Mn)	ΔE_{total} (eV)
Cubic	FM	2.67	−0.64
Cubic	AF_G	2.55	−0.84
Orthorhombic	FM	2.61	−0.31
Orthorhombic	AF_A	2.54	−0.35
Orthorhombic	AF_C	2.47	−0.44
Orthorhombic	AF_G	2.44	−0.44
Cubic-LDA calculation [6]	AF_G	2.48	
neutron diffraction [4]	—	2.65	

the ground state structure, in agreement with experimental data [4] and previous LDA calculations [6].

3.2. *CaO*(*CaMnO*$_3$)

For CaO($CaMnO_3$) we considered the $I4_1/acd$ tetragonal crystal structure reported by Fawcett *et al* [3]. This structure corresponds to a distortion of the ideal structure by a rotation of the octahedra in the **a**–**b** plane: the Mn–O–Mn bond angle changes from 180° to 165°. In this layered structure, the O in Ca–O layers, labelled O_1, and in perovskite cells, labelled O_2, are not equivalent.

As for the previous compound, we calculated the density of states for different magnetic configurations where the magnetic moments were kept along the *c* axis. For all the configurations the two O atoms show different densities of states reflecting their different environments: O_1 follows the Ca density of states while O_2 density of states shows similarities with both Ca and Mn densities. The calculated paramagnetic density of states of the distorted tetragonal structure is, in general, similar to that of $CaMnO_3$. The Fermi level lies in the centre of the Mn t_{2g} band, separated from the e_g band by a gap of 0.2 eV. The e_g band appears as a set of peaks above 0.7 eV. The Mn t_{2g} states form two peaks, one above and the other below E_F, however there is no gap and the number of Mn states at E_F is high. The Mn band just below the Fermi level is superimposed with a O_2 band. The O_2 2p states show important contributions with two more sets of peaks that spread between −2.7 and −1.3 eV and around −3.4 eV. The density of states of the distorted tetragonal structure for the ferro-and G-type antiferromagnetic configurations show spin splittings of 1.4 and 2.0 eV respectively. There is

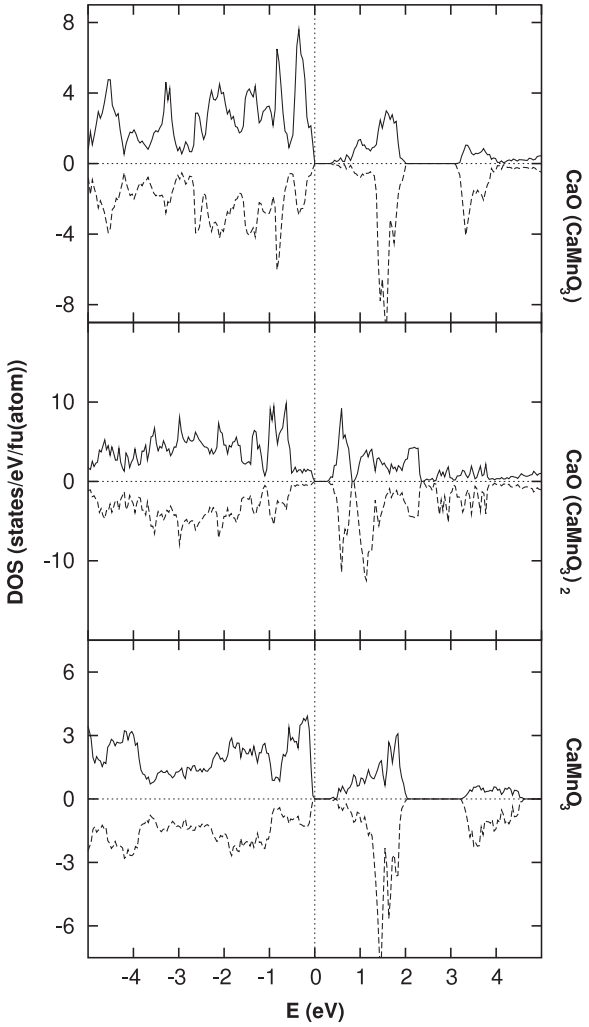

Figure 6. Total densities of states calculated for the compounds $CaO(CaMnO_3)$, $CaO(CaMnO_3)_2$ and $CaMnO_3$, for the antiferromagnetic configuration.

an insulating gap of 0.1 and 0.4 eV respectively, and in both configurations the t_{2g} states are totally polarized. The ferromagnetic configuration shows a second gap 0.2 eV above E_F. The type G antiferromagnetic tetragonal total density of states is shown in figure 6. $CaO(CaMnO_3)$ and $CaMnO_3$ G-type antiferromagnetic densities of states are similar, with similar crystal field splitting and insulating gaps and in both cases the occupied states belong mainly to Mn.

In order to study the role of the crystal structure, the antiferromagnetic density of states for a non-distorted tetragonal crystal structure (O–Mn–O bonds with 180° and 90°) was also calculated. The Mn density of states is similar to that of the distorted tetragonal structure, with the t_{2g} and e_g bands 1.4 eV apart, a spin splitting of 1.4 eV and a magnetic moment of 1.98 μ_B/Mn. However, the gap around E_F described previously is absent in this case, indicating a metallic character that contrasts with the insulating properties of the tetragonal antiferromagnetic structure.

In the paramagnetic case only Mn shows a high density of states at E_F and a significant moment in the magnetic configurations. The Mn magnetic moment, calculated with the experimental crystal structure, is close to the value found for $CaMnO_3$. The Mn moment calculated for the undistorted tetragonal structure is significantly lower and close to the neutron diffraction values [5]. The G-type antiferromagnetic configuration is 0.64 eV/f.u. lower in energy than the paramagnetic state while the ferromagnetic energy difference is 0.42 eV/f.u.

3.3. $CaO(CaMnO_3)_2$

$CaO(CaMnO_3)_2$ has a crystal structure similar to $CaO(CaMnO_3)$, with two layers of MnO_6 octahedra alternating with the CaO layers with two inequivalent Ca sites, labelled Ca_1 and Ca_2 and three O sites, labelled O_1, O_2 and O_3. The shape of the paramagnetic density of states is similar to those described for the two compounds above. The density of states at the Fermi level is high due to the Mn states with t_{2g} and e_g bands slightly overlapping. The densities of states of the different Ca and O sites clearly reflect their neighbourhoods. Ca_1 is surrounded by MnO_6 octahedra while Ca_2 belongs to the CaO layers between the perovskite blocks. Therefore Ca_1 density of states shows a maximum around E_F in the same position as a Mn maximum, absent in the Ca_2 density of states. Also the O_2 and the Mn densities of states at the Fermi level have a similar shape. The same happens with Ca_2 and O_3, located in the same plane.

The ferromagnetic density of states shows a 2 eV spin splitting of the Mn states accompanied by a small splitting in the O_1 and O_2 densities of states. The gap at the Fermi level lies at the end of the majority t_{2g} spin band. The t_{2g} minority spin band lies 0.7 eV above E_F and therefore t_{2g} is completely polarized. In order to calculate the exchange constants for the present compound, as will be presented in section 3.4, we performed calculations for two antiferromagnetic configurations: A-type antiferromagnetic in which there is a antiferromagnetic coupling between ferromagnetically ordered Mn planes; C-type antiferromagnetic, where we considered the ferromagnetic coupling between antiferromagnetic Mn planes.

The density of states calculated for the latter is presented in figure 6. The density of states is still completely polarized with a 0.4 eV gap and a spin splitting of 2 eV. This energy gap compares well with the calculated DFT/GGA (Generalized Gradient Approximation) value for the orthorhombic structure reported in [12], 0.4 eV. In comparison with the minority spin band of the other two compounds, the splitting between the e_g and t_{2g} bands is less clear and the gap above E_F that can be seen for the other two compounds is absent in the present case.

The Mn magnetic moment ranges from 2.54 to 2.70 μ_B/Mn (table 3), again lower than expected for Mn^{4+}, and the ground state configuration is an insulating antiferromagnetic structure. These values are close to the calculated moments for $CaO(CaMnO_3)_2$ within the DFT/GGA approximation [12].

3.4. Estimate of the exchange interaction

As mentioned in the previous section, for similar magnetic configurations the three compounds show similar densities of states and magnetic moments and all were found to have an

Table 2. Calculated magnetic moments and energy differences for $CaO(CaMnO_3)$ for the ferro-and antiferromagnetic configurations for the experimental tetragonal structure [3].

Magnetic structure	m (μ_B/Mn)	ΔE_{total} (eV)
FM	2.64	−0.42
AF	2.48	−0.64
Exp. [11]	1.1	—
Exp. [5]	2.0	—

Table 3. Magnetic moment and energy differences with respect to the paramagnetic configuration, calculated for $CaO(CaMnO_3)_2$: AF_A, antiferromagnetic coupling between ferromagnetically ordered Mn planes; AF_C, ferromagnetic coupling between antiferromagnetic Mn planes.

	m (μ_B/Mn)	ΔE (eV)
FM	2.70	−0.56
AF_A	2.66	−0.54
AF_C	2.54	−0.69

Table 4. Exchange constants and transition temperatures calculated for the compounds $CaMnO_3$, $CaO(CaMnO_3)$ and $CaO(CaMnO_3)_2$.

	J_{ab} (meV)	J_{c1} (meV)	J_{c2} (meV)	T_N (K)
$CaMnO_3$	9.58	8.84	—	434
$CaO(CaMnO_3)$	10.5	—	2.2	457
$CaO(CaMnO_3)_2$	17.2	0	0	534

antiferromagnetic insulating ground state. The experimental data also indicate similarities in the ground state magnetic configurations and in the transition temperatures (T_C) that prevail even if the crystal structure, and therefore the number of atoms mediating the Mn interaction, are different. In order to understand the effect of the composition on these properties we used a very simple model to calculate T_C for the three compounds. The purpose is not the calculation of realistic values but to compare the magnitude of the Mn–Mn exchange interaction between atoms in different crystal sites. Using the Heisenberg exchange Hamiltonian:

$$H = -\sum_{ij} J_{ij} S_i \cdot S_j \tag{1}$$

and separating, for example, the exchange constants for interactions within the **a**–**b** plane, J_{ab}, and along the **c** axis, J_c, one can write the total energy as:

$$E_{total} = +n_{ab} J_{ab} + n_c J_c \tag{2}$$

were n_{ab} and n_c are the number of neighbours within the **a**–**b** plane and the **c** axis. The antiferromagnetic interaction, in this model, differs from the ferromagnetic just in the sign of the exchange interaction. In this way it is possible to calculate the exchange constants through the difference of the total energy between different magnetic configurations. Assuming J_{ab} and J_c are always positive, the magnetic energy of a ferromagnetic configuration is given by

$$E_{total}(FM) = +n_{ab} J_{ab} + n_c J_c \tag{3}$$

and for an A-type antiferromagnetic configuration in which the moments aligned ferromagnetically in the basal plane it is given by

$$E_{total}(AF_A) = +n_{ab} J_{ab} - n_c J_c. \tag{4}$$

The energy difference between the two configurations can be used to calculate J_c:

$$\begin{aligned} &E_{total}(FM) - E_{total}(AF_A) \\ &= +n_{ab} J_{ab} + n_c J_c - (+n_{ab} J_{ab} - n_c J_c) \\ &= 2 n_c J_c. \end{aligned} \tag{5}$$

If one considers a third configuration, for example a G-type antiferromagnetic configuration, it is possible to calculate J_{ab}. The transition temperature, according to the mean field model, is given by the sum of the exchange constants between the atom in a position with a label 0 and the atoms in the other positions j, in the following way:

$$k_B T_C = \tfrac{2}{3} \sum_{j \neq 0} J_{0j}. \tag{6}$$

The exchange constants, determined using the energy values of tables 1–3, are summarized in table 4.

In the present work only the nearest neighbours were considered, distinguishing between the neighbours within the **a**–**b** plane and along the **c** direction. The exchange interactions between Mn in the basal plane and along the **c** axis were denoted respectively by J_{ab} and J_{c1} for Mn in the same perovskite block. The exchange interaction along the **c** axis for Mn in different perovskite blocks is denoted by J_{c2}.

The calculated values of J_{ab} and J_c for $CaMnO_3$, which has an almost cubic structure, are similar. On the other hand, J_{ab} for $CaO(CaMnO_3)$ is much larger than J_c. This is explained by the fact that the distance between consecutive Mn planes, 6.56 Å, is approximately twice the in-plane distance between Mn atoms, 3.67 Å. For $CaO(CaMnO_3)_2$ we considered two different exchange constants along **c**, J_{c1} for Mn within the same perovskite block and J_{c2} representing the exchange interaction between Mn in consecutive perovskite blocks. Again, explained by the different distances between the respective Mn atoms, J_{ab} is much larger than J_{c2}, which has a negligible value. The fact that this compound has two non-equivalent Mn sites, and that the distances between the second nearest neighbours along the **a**–**b** plane are shorter than the distances between Mn ions in consecutive perovskite blocks probably makes the simple model used here less adequate in the study of this compound. But even with such a crude method in which only the first neighbours are considered we are able to distinguish the in-plane and between plane contributions for the exchange interaction.

The computed exchange constants reproduce the expected two-dimensional (2D) character of the $CaO(CaMnO_3)$ and $CaO(CaMnO_3)_2$ compounds and therefore the use of mean field theory within the three-dimensional Heisenberg model is

Table 5. Magnetic moment and gap energies from the antiferromagnetic configurations for $CaO(CaMnO_3)$, $n = 1$, $CaO(CaMnO_3)_2$, $n = 2$ and $CaMnO_3$, $n = \infty$. H_{cryst} is t_{2g} and e_g splitting due to the crystal field.

n	m_{theory} (μ_B/Mn)	m_{exp} (μ_B/Mn)	H_{cryst} (eV)	gap_{theory} (eV)	gap_{exp} [3] (eV)
1	2.48	1.1 [11]/2.0 [5]	1.6	0.4	0.14
2	2.51	—	2.0	0.4	0.134
3	—	—	—	—	0.0966
∞	2.55	2.48 [6]/2.65 [4]	2.7	0.4	0.0618

questionable. We will, however, continue the discussion of the computed temperature values within this approximation to allow a comparison along the series. The calculated ordering temperature is similar for $CaO(CaMnO_3)$ and $CaMnO_3$. This fact agrees with experimental measurements, showing that, in the case of $CaO(CaMnO_3)$, the exchange interactions are stronger, compensating the lower number of Mn neighbours due to the large distance between Mn along the **c** plane.

The J_{ab} for $CaO(CaMnO_3)_2$ is more than one and a half times the value found for the two other compounds which leads to a transition temperature 16% higher than for $CaMnO_3$ contrary to what would be expected. Also the transition temperatures estimated for all compounds are above 400 K, higher than the experimental ordering temperatures, around 100 K [3].

4. Conclusions

The compounds $CaO(CaMnO_3)$, $CaO(CaMnO_3)_2$ and $CaMnO_3$ have, according to the present results, antiferromagnetic insulating ground state structures. The densities of states shown in figure 6 are similar for the three compounds, except for some details. The first two compounds are formed by alternating layers of CaO between the MnO_6 octahedra, therefore the densities of states of non-equivalent O atoms, located in CaO planes and perovskite blocks, reflect, respectively, the Ca and Mn neighbourhood. In the paramagnetic density of states, the number of Mn states in the Fermi level is high and results in a spin splitting that can be seen in the density of states for the magnetic states. The magnetic moment determined for the different antiferromagnetic configurations is similar for the three compounds and around 2.5 μ_B/Mn, close to the values previously determined experimentally for $CaMnO_3$.

The crystal field splitting of the e_g–t_{2g} states, as determined by the positions of the band centres in the paramagnetic states, are found to be 1.6, 2.0 and 2.7 eV, respectively, for $CaO(CaMnO_3)$, $CaO(CaMnO_3)_2$ and $CaMnO_3$. The increase of the splitting with n is related to the decrease of the distortion of the octahedra, stronger in the case of $CaO(CaMnO_3)$ and almost vanishing in the $CaMnO_3$ case.

The study of the effect of the crystal structure distortion confirms this conclusion. Although there are no significant differences between the density of states and therefore in the electronic properties of the $CaMnO_3$ orthorhombic and cubic structures, for $CaO(CaMnO_3)$ a rather different behaviour is observed. The calculations for the non-distorted structure show a metallic character in contrast to the insulating character of the experimental tetragonal crystal structure. This also indicates that the crystal structure distortion plays a more important role for the latter compound than for $CaMnO_3$.

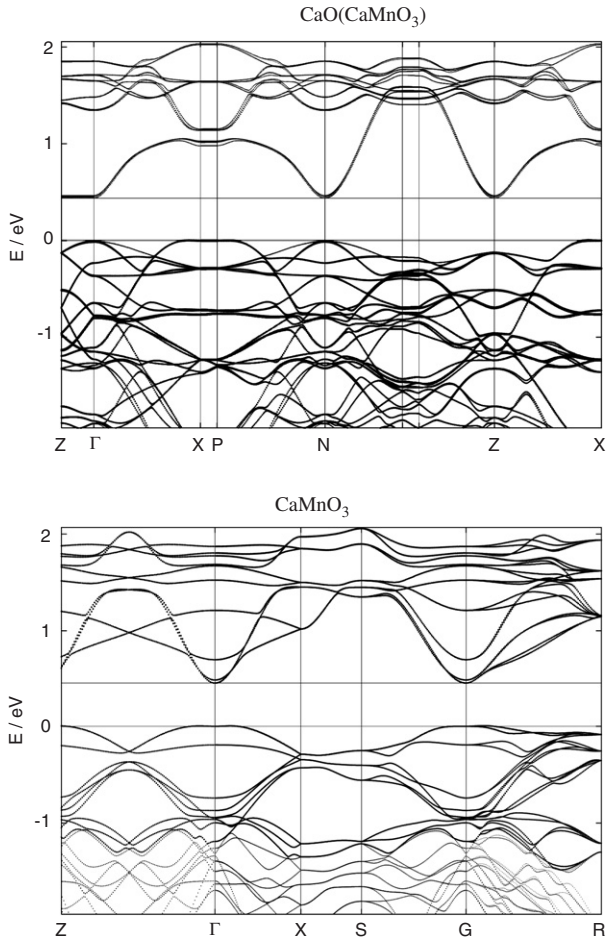

Figure 7. $CaO(CaMnO_3)$ (upper figure) and $CaMnO_3$ (lower figure) band structure calculated for the experimental antiferromagnetic configurations.

The ground state antiferromagnetic configuration presents a band gap of similar width for all the three compounds, 0.4 eV. Although it is expected that LDA calculations underestimate the gap, the calculated values are larger than the ones presented in [3] and the $CaO(CaMnO_3)_2$ value compares well with the calculated DFT/GGA value for the orthorhombic structure reported in [12]. The experimental trend reported in [3] corresponds to a decrease of the gap width with increasing n (table 5). Although these properties are very sensitive to the presence of defects such as oxygen holes, the Mn valency determined experimentally for the three compounds ranges from 3.96 to 4.02, very close to the ideal value of 4. However, other experimental reports for similar compounds indicate that the band gap should be around 3–4 eV [13–15].

Experimental work has previously focused on the transition from three-dimensionality to two-dimensionality as one goes from $CaMnO_3$ to $CaO(CaMnO_3)$. Figure 7 shows the band structures calculated for these two compounds, $CaO(CaMnO_3)$ and $CaMnO_3$. When comparing the band structures for $CaMnO_3$ and $CaO(CaMnO_3)$, the extreme flatness of the bands along the lines Z–Γ and X–P is quite

clear for the latter case, confirming the tendency from three-dimensionality in $CaMnO_3$ to two-dimensionality in $CaO(CaMnO_3)$. The calculated band widths, as defined by the difference in energy between the wavefunctions whose logarithmic derivative D at the edge of the atomic sphere is given by $D = 3$ and $D = -4$, are 5.4 eV for $CaMnO_3$ and $CaO(CaMnO_3)$ and 5.8 eV for $CaO(CaMnO_3)_2$. This is in agreement with the fact that, although the number of Mn nearest neighbours changes, the number of O nearest neighbours is constant and the Mn–O distances are similar. Therefore the present calculations confirm the trend from three-dimensionality to two-dimensionality in the band structure of these compounds but indicate that this is not directly translated into a reduction in the band width, as can be seen by the fact that the band width is greatest for the middle compound, $CaO(CaMnO_3)_2$.

Within a simple model it was also possible to calculate the exchange constants and the transition temperatures for the three compounds. Although the absolute T_C values obtained are far from the experimental values, for the reasons discussed above, this study enables us to distinguish between the in-plane and between plane exchange interactions and again reproduces a tendency to two-dimensionality for $CaO(CaMnO_3)_2$ and $CaO(CaMnO_3)$. Furthermore, by treating the three compounds on an equal footing, calculations find that the sum of the exchange interactions and consequent deduced transition temperature, are greatest for $CaO(CaMnO_3)_2$ (which also has the greater band width), and stronger for $CaO(CaMnO_3)$ than for $CaMnO_3$, as suggested by Goodenough [7]. However, we do not find it necessary to invoke a transition from itinerant to localized electrons to reproduce this finding.

Acknowledgments

This work was financed by the Portuguese Foundation for Science and Technology (FCT) through project PPCDT/FIS/60153/2004.

References

[1] Mitchell J F, Argyriou D N, Berger A, Grey K E, Osborn R and Welp U 2001 *J. Phys. Chem.* B **105** 10732
[2] Coey J M D, Viret M and von Molnar S 1999 *Adv. Phys.* **48** 167
[3] Fawcett I D, Sunstrom J E IV, Greenblatt M, Croft M and Ramanujachary K V 1998 *Chem. Mater.* **10** 3643
[4] Wollan E O and Koehler V C 1955 *Phys. Rev.* **100** 545
[5] Cox D E, Shirane G, Birgeneau R J and McChesney J B 1969 *Phys. Rev.* **188** 930
[6] Picket W E and Singh D S 1996 *Phy. Rev.* B **53** 1146
[7] Goodenough J B 1967 *Phys. Rev.* **164** 785
[8] Fawcett I D, Kim E, Greenblatt M, Croft M and Bendersky L A 2000 *Phys. Rev.* B **62** 6485
[9] Sandratskii L M 1998 *Adv. Phys.* **47** 91
[10] Kübler J 2001 *Theory of Itinerant Electron Magnetism* (Oxford: Oxford University Press)
[11] Tezuka K, Inamura M, Hinatsu Y, Shimojo Y and Morii Y 1999 *J. Solid State Chem.* **145** 705
[12] Matar S F, Eyert V, Villesuzanne A and Whangbo M-H 2007 *Phys. Rev.* B **76** 054403
[13] Jaime M, Salamon M B, Rubinstein M, Treece R E, Horwitz J S and Chrisey D B 1996 *Phys. Rev.* B **54** 11914
[14] Jung J H, Kim K H, Eom D J, Noh T W, Choi E J, Jaejun Yu, Kwon Y S and Chung Y 1997 *Phys. Rev.* B **55** 15489
[15] Zampieri G, Prado F, Caneiro A, Briático J, Causa M T, Tovar M, Alascio B, Abbate M and Morikawa E 1998 *Phys. Rev.* B **58** 3755